Molecular Therapy
Nucleic Acids
Original Article

Efficient Generation of Pathogenic A-to-G Mutations in Human Tripronuclear Embryos via ABE-Mediated Base Editing

Guanglei Li,[1,7] Xinyi Liu,[2,7] Shisheng Huang,[3,7] Yanting Zeng,[1] Guang Yang,[3] Zongyang Lu,[3] Yu Zhang,[3] Xu Ma,[4] Lisheng Wang,[2] Xingxu Huang,[3,5,6] and Jianqiao Liu[1]

[1]Department of Reproductive Medicine, Third Affiliated Hospital of Guangzhou Medical University, Guangzhou 510150, China; [2]Department of Gastroenterology, Second Clinical Medical College, Jinan University, Shenzhen People's Hospital, Shenzhen, Guangdong 510632, China; [3]School of Life Science and Technology, ShanghaiTech University, 100 Haike Road, Pudong New Area, Shanghai 201210, China; [4]National Research Institute for Family Planning, No. 12 Dahuishi Road, Beijing 100081, China; [5]CAS Center for Excellence in Molecular Cell Science, Shanghai Institute of Biochemistry and Cell Biology, Chinese Academy of Sciences, Shanghai 200031, China; [6]University of Chinese Academy of Sciences, 320 Yueyang Road, Shanghai 200031, China

Base editing systems show their power in modeling and correcting the pathogenic mutations of genetic diseases. Previous studies have already demonstrated the editing efficiency of BE3-mediated C-to-T conversion in human embryos. However, the precision and efficiency of a recently developed adenine base editor (ABE), which converts A-to-G editing in human embryos, remain to be addressed. Here we selected reported pathogenic mutations to characterize the ABE in human tripronuclear embryos. We found effective A-to-G editing occurred at the desirable sites using the ABE system. Furthermore, ABE-mediated A-to-G editing in the single blastomere of the edited embryos exhibited high product purity. By deep sequencing and whole-genome sequencing, A or T mutations didn't increase significantly, and no off-target or insertion or deletion (indel) mutations were detected in these edited embryos, indicating the ABE-mediated base editing in human embryos is precise and controllable. For some sites, since a different editing pattern was obtained from the cells and the embryos targeted with the same single guide RNA (sgRNA), it suggests that ABE-mediated editing might have different specificity *in vivo*. Taken together, we efficiently generated pathogenic A-to-G mutations in human tripronuclear embryos via ABE-mediated base editing.

INTRODUCTION

Next-generation sequencing technology has greatly advanced the discovery of pathogenic mutations in humans. Consequently, the therapeutic approaches have become the focus of modern human genetic research. Gene therapy has been considered as the most desirable strategy for repairing pathogenic mutations in human genetic diseases. Unfortunately, it was very difficult to correct these pathogenic mutations until the arrival of the revolutionary CRISPR/Cas9 technology.[1–4] Nevertheless, it is of great concern that CRISPR targeting is uncontrollable with insertion or deletion (indel) mutations.[5] A cytosine base editor (BE3/BE4) opens the potential of gene therapy by precise base editing in different species, including plant[6] and mouse,[7] and even in humans.[8–10] However, its potential is limited by the fact that CBEs (cytosine base editors) only convert the C to T and possibly induce off-target by using APOBEC.[11,12] A recently developed adenine base editor (ABE) system that converts A to G with the action of an engineered adenine deaminase ecTadA provides us another possible precise tool for gene therapy.[13,14] To demonstrate its feasibility, here we aimed to characterize the effectiveness of the ABE in human embryos.

RESULTS

The ABE System Exhibits Efficient Editing at Desirable Sites in HEK293T Cells

To comprehensively analyze the characteristics of the ABE system in human embryos, we produced the A-to-G mutation in human cells and embryos using ABE7.10. Five genes, *TTR*,[15] *ALDOB*,[16] *COL9A2*,[17] *KCNJ11*,[18] and *RPE65*,[19] which had been reported to have pathogenic A-to-G point mutations, were selected (Figure S1A). We first tested the editing of these genes with the ABE system in HEK293T cells. At 3 days after transfection of ABE7.10 with the corresponding single guide RNAs (sgRNAs) targeting these five genes individually, the genomic DNA sample was extracted from the transfected HEK293T cells, and it was used as the template to amplify the target regions by PCR. The PCR product was subjected to Sanger sequencing.

Received 16 April 2019; accepted 22 May 2019;
https://doi.org/10.1016/j.omtn.2019.05.021.

[7]These authors contributed equally to this work.

Correspondence: Jianqiao Liu, Department of Reproductive Medicine, Third Affiliated Hospital of Guangzhou Medical University, Guangzhou 510150, China.
E-mail: liujqssz@gzhmu.edu.cn
Correspondence: Xingxu Huang, School of Life Science and Technology, ShanghaiTech University, 100 Haike Road, Pudong New Area, Shanghai 201210, China.
E-mail: huangxx@shanghaitech.edu.cn
Correspondence: Lisheng Wang, Department of Gastroenterology, Second Clinical Medical College, Jinan University, Shenzhen People's Hospital, Shenzhen, Guangdong 510632, China.
E-mail: maxwangls@sina.com

Table 1. Summary of the Used Embryos Edited with ABE

			Edited Embryo			Blastomere		
				Efficiency >50%	Efficiency >80%		2 Edited Alleles	3 Edited Alleles
Serial Number of Injection	Used sgRNA		Number	Number (%)	Number (%)	Number	Number (%)	Number (%)
1	*SITE6*		12	7 (58)	3 (25)	NA		
2	*SITE2*		12	12 (100)	11 (92)	NA		
3	*ALDOB*		7	0 (0)	0 (0)	NA		
4	*COL9A2*		7	6 (86)	4 (57)	NA		
5	*KCNJ11*		7	0 (0)	0 (0)	NA		
6	*TTR*		12	12 (100)	10 (83)	NA		
7	*RPE65*		10	6 (60)	0 (0)	NA		
8	*TTR + RPE65*	*TTR*	10	10 (100)	9 (90)	NA		
		RPE65	10	9 (90)	5 (50)	NA		
9	*TTR*		6	–	–	48	46 (96)	37 (77)

NA, not applicable.

As expected, double A and double G peaks were observed in the sequencing chromatogram (Figure S1B), indicating the successful A-to-G editing of the targeted sites. Then, we further calculated the base editing efficiency for each target A site based on three independent experiments, by using the EditR software (https://moriaritylab.shinyapps.io/editr_v10/). The results showed that successful base editing was achieved at all targeted sites, but with different editing efficiencies (Figure S1C). The A-to-G conversions were further confirmed for two target sites with the highest editing efficiencies, the A_6 of *TTR* (editing efficiency, 75%) and the A_4 of *RPE65* (editing efficiency, 71%), by sequencing the PCR product derived from these two genomic DNA samples after the TA cloning (Figure S1D). It is worth noting that, besides the base editing at the desirable sites, the A_3 for *TTR* and the A_2 for *RPE65* were also edited with an efficiency of about 15% (3 in 20 clones) and 12% (2 in 17 clones), respectively. Taken together, the pathogenic A-to-G mutations of the selected genes had been successfully achieved by the ABE system in HEK293T cells.

The ABE System Efficiently Converts A to G in Discarded Human Tripronuclear Embryos

Then, we tested the ABE in discarded human tripronuclear embryos. First, two reported sgRNAs targeting *SITE2* and *SITE6*,[13] each together with mRNA of ABE7.10, were microinjected into the human tripronuclear embryos as described previously.[9] 3 days later, 12 embryos for each site were obtained for genotyping by Sanger sequencing of the PCR product (Table 1). The editing efficiency was calculated by using EditR (Table S1). The results showed that the A_7 of *SITE6* was efficiently edited in all embryos. Meanwhile, A_3 editing was observed at *SITE6* in some embryos (6, 8, and 9). For *SITE2*, A_5 was efficiently edited in all samples, and A_2 editing and A_8 editing were also detected in several embryos (21 and 22). Notably, editing occurred in most of the *SITE2* samples (92%) at an efficiency of more than 80% (Table 1).

To further test the base conversion efficiency, the DNA samples targeting *SITE6* in five embryos (5–7, 9, and 12) and targeting *SITE2* in five other embryos (13, 14, and 17–19) were randomly selected for deep sequencing (Table S1). Then, the editing efficiency was measured for all As 10 bp upstream of the sgRNA target region as well as within the sgRNA region. We consistently observed that the A_5 of *SITE2* and the A_7 of *SITE6* were edited with the highest efficiencies. In addition, low levels of editing were observed at the A_8 and the A_2 of *SITE2* and the A_3 of *SITE6* (Figure 1A). No editing occurred at any other sites. Taken together, we achieved efficient A-to-G editing in human embryos with ABE7.10.

Furthermore, the editing at *TTR* and *RPE65* was tested in 12 and 10 respective human tripronuclear embryos, as described above (Table 1). Sanger sequencing of the PCR product showed that the A-to-G conversion occurred in most of the embryos at the pathogenic mutation sites with A_6 for *TTR* and A_4 for *RPE65*, respectively (Table S1). Similarly, some embryos (embryos 47–49, 51, and 53 for *TTR* and embryos 58, 60, and 64–66 for *RPE65*) were randomly selected for deep sequencing to further characterize the editing efficiencies and specificities. We consistently observed efficient editing at the A_6 of *TTR* and the A_4 of *RPE65*. Low levels of editing were observed at the A_3 of *TTR* and the A_2 of *RPE65* (Figure 1B). Based on the deep sequencing results of the above 4 target sites, ABE induces the best base editing efficiencies at the positions 4–7 of the protospacer region in human embryos (Figure 1C). Editing at A_3 was also observed, as has been reported before.[13] Meanwhile, we also analyzed the fractions of adenine substitutions for the efficiently edited sites of *SITE2*, *SITE6*, *TTR*, and *RPE65*. Indeed, almost all of the conversions were A to G (Figure 1D), indicating that the ABE system produces highly pure products in human embryos. We also analyzed the indels for *TTR* and *RPE65* and, as expected, no indel was detected (Figure S2).

Sometimes it is necessary to model multiple pathogenic mutations, so we tried to simultaneously edit multiple sites by ABE. Similar to what

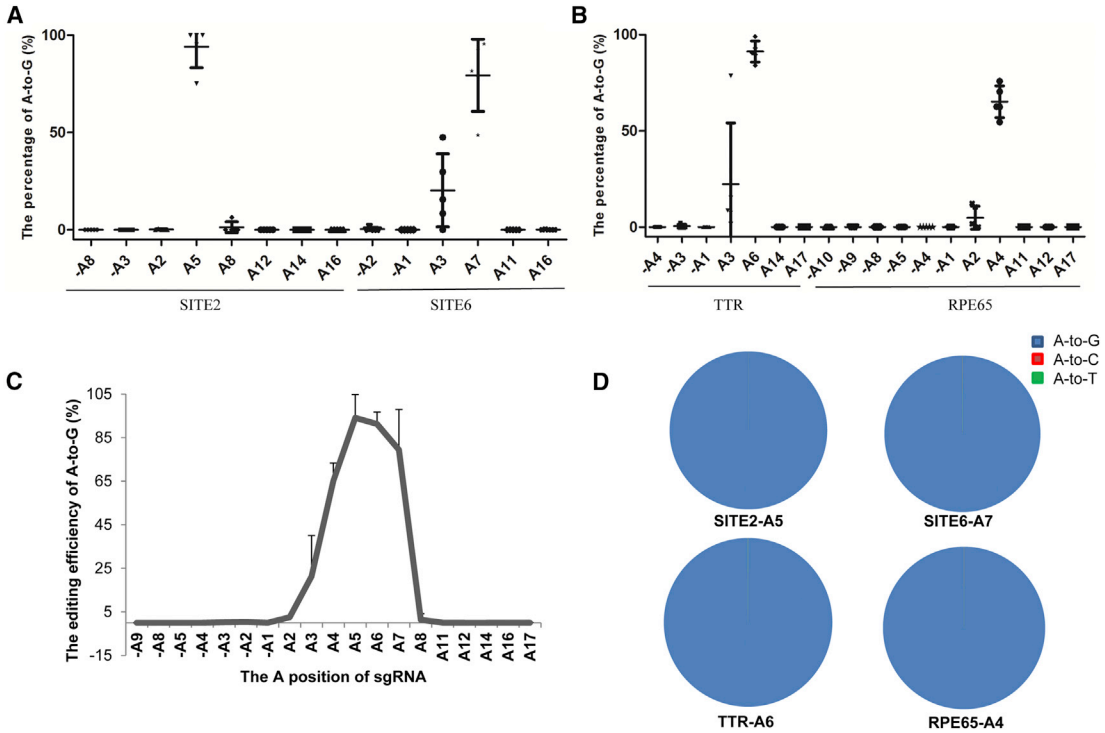

Figure 1. Generation of Specific Pathogenic Point Mutations in Human Tripronuclear Embryos Using the ABE System

(A) Analysis of the ABE-mediated A-to-G editing of the reported sites in human embryos by deep sequencing. Two reported sites (SITE2 and SITE6) were selected to test the A-to-G editing in human tripronuclear embryos. The editing of all A sites 10 bp upstream of the sgRNA and within the sgRNA was analyzed by deep sequencing. Data of the detected embryos described in Table S1 are shown as the mean ± SD (n = 5). (B) Analysis of ABE-mediated A-to-G editing of the novel sites in human embryos by deep sequencing. Two novel sites, *TTR* and *RPE65*, were selected for A-to-G editing in human tripronuclear embryos. The editing of all the A sites 10 bp upstream and within the sgRNA was analyzed by deep sequencing. Data of the detected embryos described in Table S1 are shown as the mean ± SD (n = 5). (C) Characterization of the ABE-mediated A-to-G substitution at different positions in human tripronuclear embryos. (D) Analysis of different adenine substitutions of the target sites. The positions with most efficient editing of the 4 target sites were selected for analysis.

was described in BE3-mediated multiple C-to-T conversions,[9] we simultaneously microinjected two sgRNAs, *TTR* and *RPE65*, into 10 embryos (Table S1). After sequencing, the editing efficiencies at the desirable A_6 of *TTR* and A_4 for *RPE65* were 91% and 70%, respectively (Figure S3A). To further characterize the editing efficiencies of multiple sites in human embryos, five embryos (70, 72, 74, 76, and 77) were randomly selected for deep sequencing. Analysis of the deep sequencing data showed that simultaneous editing by ABE produces similar editing efficiencies and patterns at both *TTR* and *RPE65* (Figure S3B), suggesting that the ABE system could be used to manipulate multiple pathogenic point mutations with high efficiency and accuracy.

The Editing Characteristic in Embryos Is Different from that in 293T Cells for Some Sites

Next, three targets, *ALDOB*, *COL9A2*, and *KCNJ11*, with poor editing in HEK293T cells were tested for the editing efficiencies in human embryos. Each sgRNA together with mRNA of ABE7.10 was microinjected into 7 tripronuclear embryos, respectively (Table 1). We found the sgRNAs of *ALDOB* and *KCNJ11* still gave rise to low base conversion efficiencies in human tripronuclear embryos, similar to those observed in HEK293T cells (Figure S4). However, *COL9A2* showed highly efficient editing at A_8 in human tripronuclear embryos (Figure 2A), which was hardly detectable in HEK293T cells (Figure S1C), indicating the differences of ABE-mediated base editing between cells and embryos. Moreover, we found 2 other sites (*BCS1L-1* and *BCS1L-2* sites) using the ABE-NG system that recognized the non-NGG protospacer adjacent motif (PAM) sequences (Figure 2B). The analysis confirmed the differences of ABE-mediated base editing between cells and embryos (Figures 2C and 2D).

Analysis of Blastomeres for TTR-Edited Embryos

As described above, deep sequencing analysis proves the efficiency and product purity of ABE-mediated base editing in human embryos. This suggests that there is only a low level of other kinds of genotypes in ABE-mediated base editing. To further address this concern, we performed the genotyping analysis for every single blastomere of the edited embryos (Figure 3A). The blastomeres collected from 6 *TTR*-edited embryos were used for genotyping (Figure 3B). The results showed that the base substitutions occurred at pathogenic A_6 with nearly perfect efficiencies for three *TTR* alleles in every triploid blastomere of the edited embryos (78, 95%; 79, 96%; 80, 80%; 81,

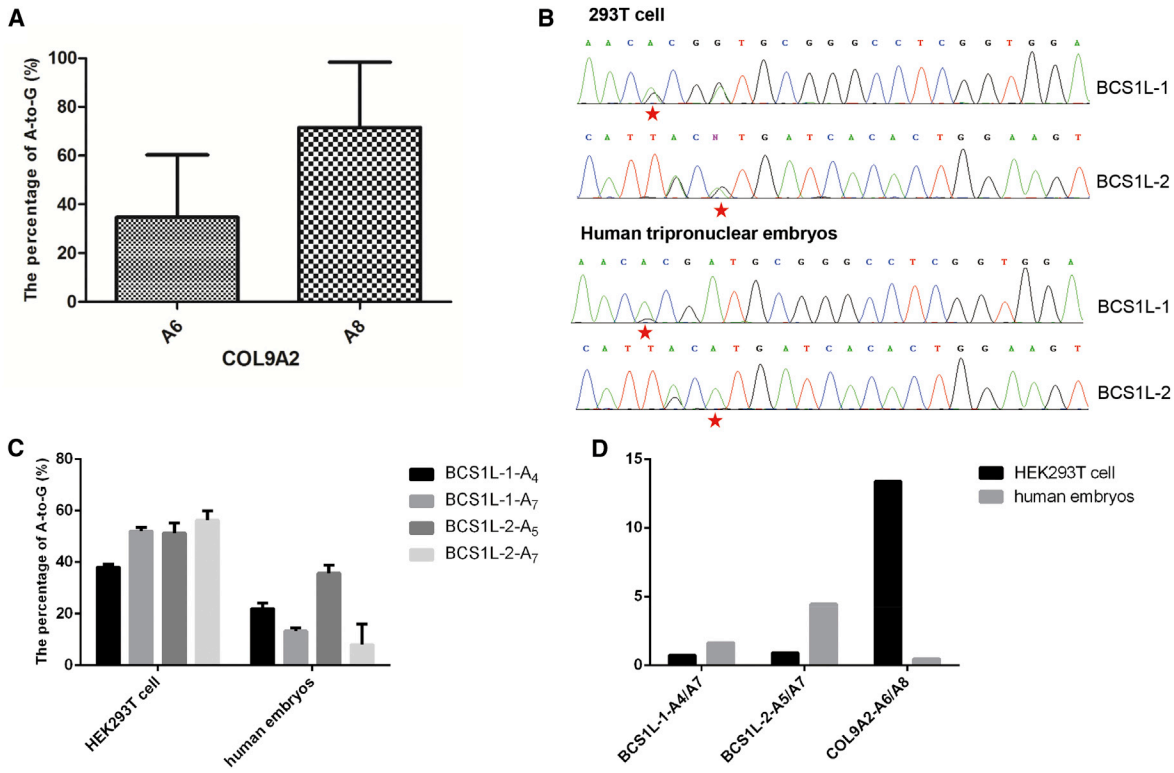

Figure 2. The Editing Characteristic in Embryos Is Different from that in 293T Cells

(A) The editing efficiency of A6 and A8 for the COL9A2 gene in embryos was calculated. Data from three independent experiments are shown as means ± SD. (B) Two target sequences that contained the GGA or AGT PAM were edited using ABE-NG. The representative chromatograms of the Sanger sequencing of target sites from genomic DNA of HEK293T cells (top) and human tripronuclear embryos (bottom) are shown. The red star indicates the pathogenic point. (C) The A4 and A7 sites for the BCS1L-1 gene site were calculated by EditR software via Sanger sequencing of the PCR products derived from the target sites. Data are shown as the mean ± SD (n = 3). The A5 and A7 sites for the BCS1L-2 gene site were calculated with the same method. (D) The ratios of editing efficiency for different points of the three gene sites were calculated using the previous data.

100%; 82, 87%; and 83, 89%) (Figure 3C), indicating the ABE-mediated base editing in human embryos is controllable.

Off-Target Analysis by Deep Sequencing and Whole-Genome Sequencing

Another concern about genome editing is the off-target base editing.[20] To explore the off-target edited sites of ABE in human embryos, the potential off-target sites of the sgRNAs for *TTR* and *RPE65* were predicted by using three different available tools.[21–23] In total, there were 21 predicted potential off-target sites of the *TTR* sgRNA (Table S2) and 23 off-target sites of the *RPE65* sgRNA (Table S3). Then, 10 edited embryos (68–77) were used for the detection of the off-target sites, with 5 embryos injected with the ABE mRNA and the scramble sgRNA as the control. The PCR products of all edited embryos were mixed with an equal amount of DNA for each embryo and subjected to deep sequencing. The results showed that there were no obviously detectable off-target sites (Figure 4A).

To further demonstrate the fidelity of ABE-mediated base editing in human embryos, we performed whole-genome sequencing (WGS) on genomic DNA isolated from 2 control embryos, TTR-53 and RPE65-65, at the depth of 30–40×. Totals of 237,605 sites for RPE65 and 536,022 sites for TTR, with up to 5-bp mismatches and equal or less than one DNA or RNA bulge in the sgRNA-targeting region, were analyzed. After excluding the false-positive sites depending on The Single Nucleotide Polymorphism Databases (dbSNPs), the mutation frequency of A or T didn't seem to increase significantly, and no off-target was uniquely assigned to both tested samples (Figure 4B). These results indicated that ABE can mediate precise base editing with high efficiency and fidelity in human embryos.

DISCUSSION

For human genetic diseases, gene therapy has become an ideal alternative strategy to prevent the germline transmission of the founder mutations. To date, there are about 10,000 reported monogenic inherited mutations that may be generated by precise gene-editing technologies. Previously, we have reported the success to precisely convert C to T in human embryos by using a cytosine base editor. However, nearly 50% of pathogenic point mutations were caused by G-to-A conversion instead.[13] The newly developed ABE, which converts A to G, provides a potential tool for creating these pathogenic mutations. To test its potential, we performed the ABE-mediated A-to-G

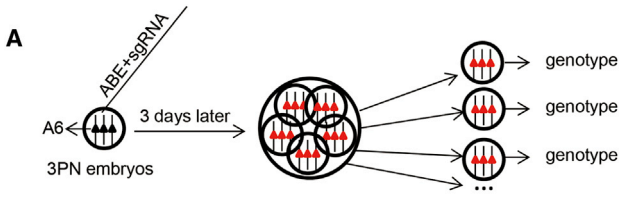

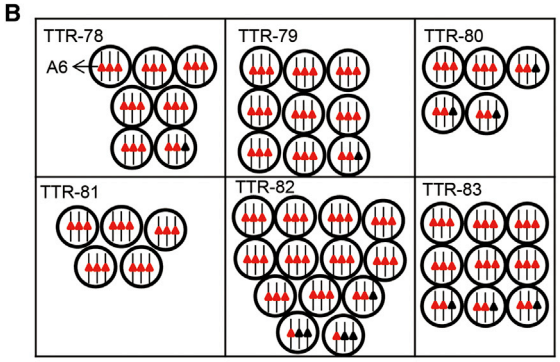

C

	Alleles	Edited alleles	Efficiency
TTR-78	21	20	95%
TTR-79	27	26	96%
TTR-80	15	12	80%
TTR-81	15	15	100%
TTR-82	39	34	87%
TTR-83	27	24	89%
Total	144	131	91%

Figure 3. Analysis of ABE-Mediated Base Editing of the *TTR* Gene in Blastomeres

(A) Schematic illustration of the experimental procedure for analysis of ABE-mediated base editing in triploid blastomeres. A6 in the target sites was detected. Each string presents one allele in the tripronuclear embryos. The black triangle means adenine and the red triangle means guanine. The genotype was calculated via Sanger sequencing of the target sites. (B) Six embryos for the *TTR* gene were divided into triploid blastomeres. Each box indicates one embryo. The black triangle means adenine and the red triangle means guanine. (C) Summary of the alleles with the edited A_6 site in triploid blastomeres.

editing by microinjection of ABE mRNA together with target sgRNA. As expected, we observed efficient ABE-mediated A-to-G conversion.

Off-target is rare with base editors.[5] Indeed, A or T mutations didn't increase significantly, and no obvious off-target sites were observed in the edited human embryos by ABE based on thorough deep sequencing and whole-genome sequencing analysis, further evidence for BEs as the safe genome editors.[24] More interestingly, no other base conversions (A to C or A to T) were induced by ABE, although there was low level of A-to-G conversion at the undesirable sites. This kind of undesirable A-to-G conversion may be prevented by other means, such as the use of different sgRNAs or Cas9. It is worth noting that the ABE-mediated editing showed different editing patterns between HEK293T cells and human embryos for some sites, indicating different specificity of ABE-mediated editing *in vivo* compared with that in cells. We found 77% (37/48) of the blastomeres harbored the same base conversion at the pathogenic site (Table 1); no other genotype was found, suggesting that ABE-mediated editing is more controllable. Nevertheless, whether a ribonucleoprotein (RNP) system and metaphase II (MII) oocyte injection can further increase the efficiency of base editing need to be tested.[25]

In summary, we successfully achieved and characterized the ABE-mediated editing in human embryos. The results demonstrated that ABE-mediated base editing was efficient and precise, providing a novel strategy for modeling and correcting the pathogenic G-to-A point mutation.

MATERIALS AND METHODS

Discarded Human Tripronuclear Zygotes

The study was approved by the Ethics Committee of the Third Affiliated Hospital of Guangzhou Medical University. All of the used tripronuclear zygotes were donated by the patients undergoing *in vitro* fertilization (IVF) treatment at the Center for Reproductive Medicine of the hospital. The patients signed the informed consent before sample collection.

Plasmid Construction and *In Vitro* Transcription

The sequence of ABE7.10 was synthesized and cloned into mammal expression plasmid with cytomegalovirus (CMV) or T7 promoter. We replaced the puromycin element of pGL3-U6-sgRNA-phosphoglycerate kinase (PGK)-puromycin (Addgene, 51133) with the GFP sequence to produce the pGL3-U6-sgRNA-PGK-GFP plasmid. The oligos for the used sgRNAs were synthesized and respectively cloned into the pGL3-U6-sgRNA-PGK-GFP vector and pUC57-sgRNA expression vector (Addgene, 51132). All of the plasmids were extracted and quantified with Nanodrop 2000. The pGL3-U6-sgRNA-PGK-GFP plasmids were used to transfect into the HEK293T cells. The pUC57-sgRNA plasmids were used as the template for *in vitro* transcription. The ABE was transcribed *in vitro* according to the reported protocol.[9] Briefly, the plasmid was digested using BbsI and then was purified using a PCR clean-up kit (Axygene, AP-PCR-250). The linearized plasmid was used as the template to generate the mRNA transcript. The sgRNA was transcribed according to the reported protocol.[9] The concentration of the transcribed RNA was measured with Nanodrop 2000, and the RNA samples were stored at −80°C before use for microinjection.

Cell Culture, Transfection, and Identification

HEK293T cells were maintained in DMEM-high glucose (HyClone, SH30243.01) with 10% fetal bovine serum (FBS) (v/v) (Gemini, 900-108). The ABE plasmid was transfected into the HEK293T cells with the corresponding sgRNA expression plasmid by using Lipofectamine 2000 reagent (Life Technologies), according to the manufacturer's suggested protocols. 3 days later, 50,000 GFP-positive cells were sorted using flow cytometry. The collected cells were lysed in the buffer containing 50 mM KCl, 1.5 mM $MgCl_2$, 10 mM Tris (pH 8.0), 0.5% Nonidet P-40, 0.5% Tween 20, and 100 μg/mL protease K at 65°C for 30 min. Then, the samples were heated at 98°C for 3 min. The target sequences were amplified and sequenced using the primers corresponding to each target gene (Table S4).

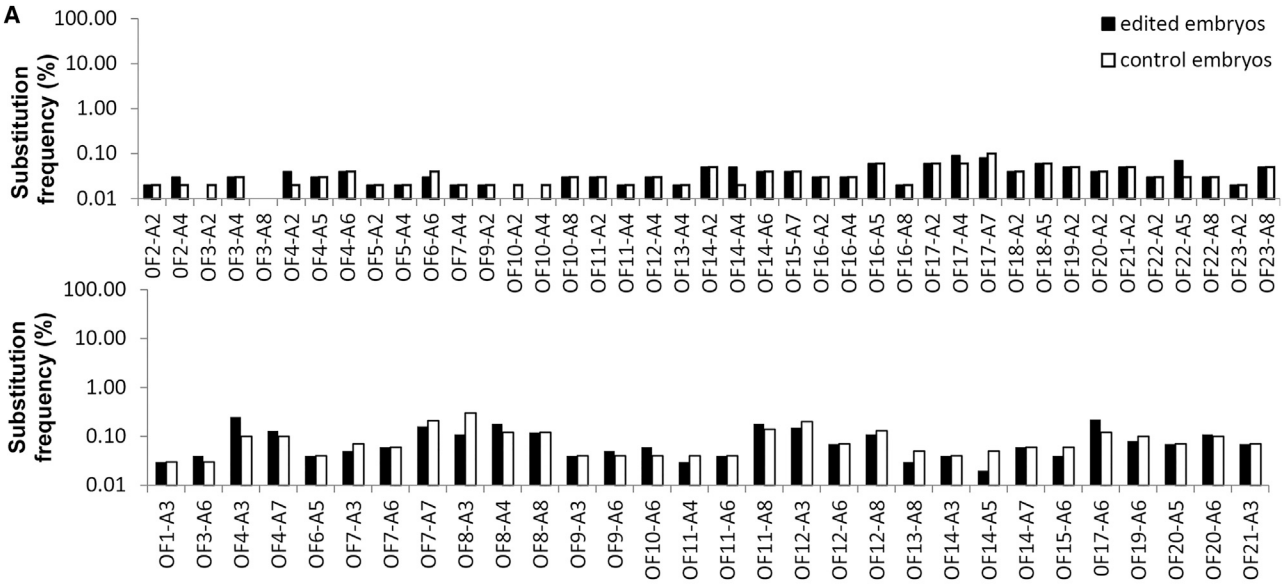

B

	Total SNPs	SNPs after excluding dbSNPs	A>G SNPs	A>C SNPs	A>T SNPs	T>C SNPs	T>G SNPs	T>A SNPs	Possible off-target for RPE65 (237605 sites)	Possible off-target for TTR(536022 sites)
Control-1	2,217,143	589,148	90,024	26,462	18,939	90,475	26,357	18,981	26	12
Control-2	2,235,681	614,848	90,349	26,408	19,098	91,128	26,095	19,199	27	12
RPE65-#65	2,271,094	654,770	90,331	26,061	18,841	90,823	25,970	18,812	24	-
TTR-#53	2,138,332	557,038	88,250	25,952	18,622	88,935	25,814	18,775	-	11
Uniquely assigned to RPE65-#65	508,038	178,042	9,207	3,349	2,668	9,235	3,342	2,669	0	-
Uniquely assigned to TTR-#53	383,493	81,945	7,567	3,341	2,542	7,550	3,138	2,518	-	0

Figure 4. Off-Target Site Analysis

(A) Totals of 23 off-target sites for *RPE65* (top) and 21 off-target sites for *TTR* (bottom) were selected. The off-target frequencies were calculated by deep sequencing. The adenine sites within the positions of 2–8 of sgRNA were examined for off-target frequencies. (B) Whole-genome-wide sequencing analysis was conducted for two control embryos and two edited embryos.

Embryo Injection and Culture

The tripronuclear zygotes were picked after 16–18 h of IVF under microscope. The RNA solution was diluted at the concentration of 100 ng/μL for ABE-generated mRNA and 50 ng/μL for sgRNA. The procedure for microinjection was the same as the reported method by using a micromanipulator (Eppendorf, Germany).[26] The embryos were kept in embryo culture medium (Vitrolife, Sweden) for 3 days. Then the whole embryos were collected for experiments, or the blastomeres were obtained from these embryos with the acidic Tyrode's solution (Solarbio, Beijing, China) before use.

Whole-Genome Amplification of Single Embryos

The collected embryos and blastomeres were amplified using Discover-sc Single Cell Kit (Vazyme, N601-01). The product was diluted 100-fold before it was used as the template to amplify the target sites.

Deep Sequencing of On-Target and Off-Target Sites

The off-target sites for *TTR* and *RPE65* were predicted by using three reported softwares (https://zlab.bio/guide-design-resources; https://crispr.cos.uni-heidelberg.de/; http://www.rgenome.net/cas-offinder/)[21–23]. The on-target and off-target sites for the edited

embryos (Table S1) were amplified using super-fidelity DNA polymerase (Vazyme, p505). The purified PCR products were submitted to sequencing using Hiseq X-10 (2 × 150) platform at CAS-MPG Partner Institute for Computational Biology Omics Core, Shanghai, China. The deep sequencing data were processed using the Burrows-Wheeler Aligner-maximal exact matches (BWA-MEMs) algorithm. The column diagram about the editing efficiency was produced using GraphPad.

Whole-Genome Sequencing for the Off-Target Detection

To comprehensively analyze the off-targets induced by ABE in human embryos, whole-genome sequencing was performed with a depth of 30×–40× using an Illumina HiSeq X Ten (2 × 150 paired end [PE]) at HuaGen Biotech Institute, Shanghai, China. BWA version (v.)0.7.16 was used to map the sequencing data with a human reference genome (GRCh38/hg38). Sequence reads were marked for duplicates using Sambamba v.0.6.7 and realigned using Genome Analysis Toolkit (GATK, v.3.7) IndelRealigner. Variants were identified by GATK HaplotypeCaller, and we evaluated the quality using GATK VariantFiltration. The putative off-target sites were obtained from Cas-OFFinder software, with up to 5 mismatches and equal or less than one DNA or RNA bulge. To figure out the potential off-target sites, A to G was picked out. The common SNPs between the edited and control embryos were discarded.

Data Availability

All the deep sequencing data can be viewed in the National Omics Data Encyclopedia (NODE) (https://www.biosino.org/node/) by pasting the accession (OEP000192) into the text search box or through the URL https://www.biosino.org/node/project/detail/OEP000192. The whole-genome sequencing data have been deposited in the NCBI Sequence Read Archive database (SRA: PRJNA480397).

SUPPLEMENTAL INFORMATION

Supplemental Information can be found online at https://doi.org/10.1016/j.omtn.2019.05.021.

AUTHOR CONTRIBUTIONS

J.L., X.H., L.W., and G.L. conceived and designed the project. G.L., X.L., S.H., Y. Zeng, G.Y., Z.L., X.M., and Y. Zhang performed the experiments. X.H., J.L., and L.W. supervised the project. X.H. and G.L. analyzed the data and wrote the paper.

CONFLICTS OF INTEREST

The authors declare no competing interests.

ACKNOWLEDGMENTS

We thank members of the Huang and Liu labs for helpful discussions. We are grateful to Dr. Xiajun Li from ShanghaiTech University for excellent language editing. This work was supported by the grants from the National Natural Science Foundation of China grant (31471400), the Provincial Major Project of Guangdong Provincial Department of Education (2014KZDXM047) and the China Postdoctoral Science Foundation (2017M622659).

REFERENCES

1. Katsanis, N. (2018). Point: Treating Human Genetic Disease One Base Pair at a Time: The Benefits of Gene Editing. Clin. Chem. *64*, 486–488.
2. Austin, C.P., and Dawkins, H.J.S. (2017). Medical research: Next decade's goals for rare diseases. Nature *548*, 158.
3. Liu, Y., Yang, Y., Kang, X., Lin, B., Yu, Q., Song, B., Gao, G., Chen, Y., Sun, X., Li, X., et al. (2017). One-Step Biallelic and Scarless Correction of a β-Thalassemia Mutation in Patient-Specific iPSCs without Drug Selection. Mol. Ther. Nucleic Acids *6*, 57–67.
4. Kang, X., He, W., Huang, Y., Yu, Q., Chen, Y., Gao, X., Sun, X., and Fan, Y. (2016). Introducing precise genetic modifications into human 3PN embryos by CRISPR/Cas-mediated genome editing. J. Assist. Reprod. Genet. *33*, 581–588.
5. Kim, D., Lim, K., Kim, S.T., Yoon, S.H., Kim, K., Ryu, S.M., and Kim, J.S. (2017). Genome-wide target specificities of CRISPR RNA-guided programmable deaminases. Nat. Biotechnol. *35*, 475–480.
6. Zong, Y., Wang, Y., Li, C., Zhang, R., Chen, K., Ran, Y., Qiu, J.L., Wang, D., and Gao, C. (2017). Precise base editing in rice, wheat and maize with a Cas9-cytidine deaminase fusion. Nat. Biotechnol. *35*, 438–440.
7. Kim, K., Ryu, S.M., Kim, S.T., Baek, G., Kim, D., Lim, K., Chung, E., Kim, S., and Kim, J.S. (2017). Highly efficient RNA-guided base editing in mouse embryos. Nat. Biotechnol. *35*, 435–437.
8. Zhou, C., Zhang, M., Wei, Y., Sun, Y., Sun, Y., Pan, H., Yao, N., Zhong, W., Li, Y., Li, W., et al. (2017). Highly efficient base editing in human tripronuclear zygotes. Protein Cell *8*, 772–775.
9. Li, G., Liu, Y., Zeng, Y., Li, J., Wang, L., Yang, G., Chen, D., Shang, X., Chen, J., Huang, X., and Liu, J. (2017). Highly efficient and precise base editing in discarded human tripronuclear embryos. Protein Cell *8*, 776–779.
10. Zeng, Y., Li, J., Li, G., Huang, S., Yu, W., Zhang, Y., Chen, D., Chen, J., Liu, J., and Huang, X. (2018). Correction of the Marfan Syndrome Pathogenic FBN1 Mutation by Base Editing in Human Cells and Heterozygous Embryos. Mol. Ther. *26*, 2631–2637.
11. Zuo, E., Sun, Y., Wei, W., Yuan, T., Ying, W., Sun, H., Yuan, L., Steinmetz, L.M., Li, Y., and Yang, H. (2019). Cytosine base editor generates substantial off-target single-nucleotide variants in mouse embryos. Science *364*, 289–292.
12. Jin, S., Zong, Y., Gao, Q., Zhu, Z., Wang, Y., Qin, P., Liang, C., Wang, D., Qiu, J.L., Zhang, F., and Gao, C. (2019). Cytosine, but not adenine, base editors induce genome-wide off-target mutations in rice. Science *364*, 292–295.
13. Gaudelli, N.M., Komor, A.C., Rees, H.A., Packer, M.S., Badran, A.H., Bryson, D.I., and Liu, D.R. (2017). Programmable base editing of A●T to G●C in genomic DNA without DNA cleavage. Nature *551*, 464–471.
14. Matsoukas, I.G. (2018). Commentary: Programmable base editing of A·T to G·C in genomic DNA without DNA cleavage. Front. Genet. *9*, 21.
15. Sekijima, Y., Campos, R.I., Hammarström, P., Nilsson, K.P., Yoshinaga, T., Nagamatsu, K., Yazaki, M., Kametani, F., and Ikeda, S. (2015). Pathological, biochemical, and biophysical characteristics of the transthyretin variant Y114H (p.Y134H) explain its very mild clinical phenotype. J. Peripher. Nerv. Syst. *20*, 372–379.
16. Esposito, G., Imperato, M.R., Ieno, L., Sorvillo, R., Benigno, V., Parenti, G., Parini, R., Vitagliano, L., Zagari, A., and Salvatore, F. (2010). Hereditary fructose intolerance: functional study of two novel ALDOB natural variants and characterization of a partial gene deletion. Hum. Mutat. *31*, 1294–1303.
17. Annunen, S., Paassilta, P., Lohiniva, J., Perälä, M., Pihlajamaa, T., Karppinen, J., Tervonen, O., Kröger, H., Lähde, S., Vanharanta, H., et al. (1999). An allele of COL9A2 associated with intervertebral disc disease. Science *285*, 409–412.
18. Gloyn, A.L., Reimann, F., Girard, C., Edghill, E.L., Proks, P., Pearson, E.R., Temple, I.K., Mackay, D.J., Shield, J.P., Freedenberg, D., et al. (2005). Relapsing diabetes can result from moderately activating mutations in KCNJ11. Hum. Mol. Genet. *14*, 925–934.

19. Felius, J., Thompson, D.A., Khan, N.W., Bingham, E.L., Jamison, J.A., Kemp, J.A., and Sieving, P.A. (2002). Clinical course and visual function in a family with mutations in the RPE65 gene. Arch. Ophthalmol. *120*, 55–61.

20. Kang, X.J., Caparas, C.I.N., Soh, B.S., and Fan, Y. (2017). Addressing challenges in the clinical applications associated with CRISPR/Cas9 technology and ethical questions to prevent its misuse. Protein Cell *8*, 791–795.

21. Stemmer, M., Thumberger, T., Del Sol Keyer, M., Wittbrodt, J., and Mateo, J.L. (2015). CCTop: An Intuitive, Flexible and Reliable CRISPR/Cas9 Target Prediction Tool. PLoS ONE *10*, e0124633.

22. Hsu, P.D., Scott, D.A., Weinstein, J.A., Ran, F.A., Konermann, S., Agarwala, V., Li, Y., Fine, E.J., Wu, X., Shalem, O., et al. (2013). DNA targeting specificity of RNA-guided Cas9 nucleases. Nat. Biotechnol. *31*, 827–832.

23. Bae, S., Park, J., and Kim, J.S. (2014). Cas-OFFinder: a fast and versatile algorithm that searches for potential off-target sites of Cas9 RNA-guided endonucleases. Bioinformatics *30*, 1473–1475.

24. Akcakaya, P., Bobbin, M.L., Guo, J.A., Malagon-Lopez, J., Clement, K., Garcia, S.P., Fellows, M.D., Porritt, M.J., Firth, M.A., Carreras, A., et al. (2018). In vivo CRISPR editing with no detectable genome-wide off-target mutations. Nature *561*, 416–419.

25. Ma, H., Marti-Gutierrez, N., Park, S.W., Wu, J., Lee, Y., Suzuki, K., Koski, A., Ji, D., Hayama, T., Ahmed, R., et al. (2017). Correction of a pathogenic gene mutation in human embryos. Nature *548*, 413–419.

26. Tang, L., Zeng, Y., Du, H., Gong, M., Peng, J., Zhang, B., Lei, M., Zhao, F., Wang, W., Li, X., and Liu, J. (2017). CRISPR/Cas9-mediated gene editing in human zygotes using Cas9 protein. Mol. Genet. Genomics *292*, 525–533.

OMTN, Volume *17*

Supplemental Information

Efficient Generation of Pathogenic A-to-G Mutations in Human Tripronuclear Embryos via ABE-Mediated Base Editing

Guanglei Li, Xinyi Liu, Shisheng Huang, Yanting Zeng, Guang Yang, Zongyang Lu, Yu Zhang, Xu Ma, Lisheng Wang, Xingxu Huang, and Jianqiao Liu

SUPPLEMENTARY INFORMATION

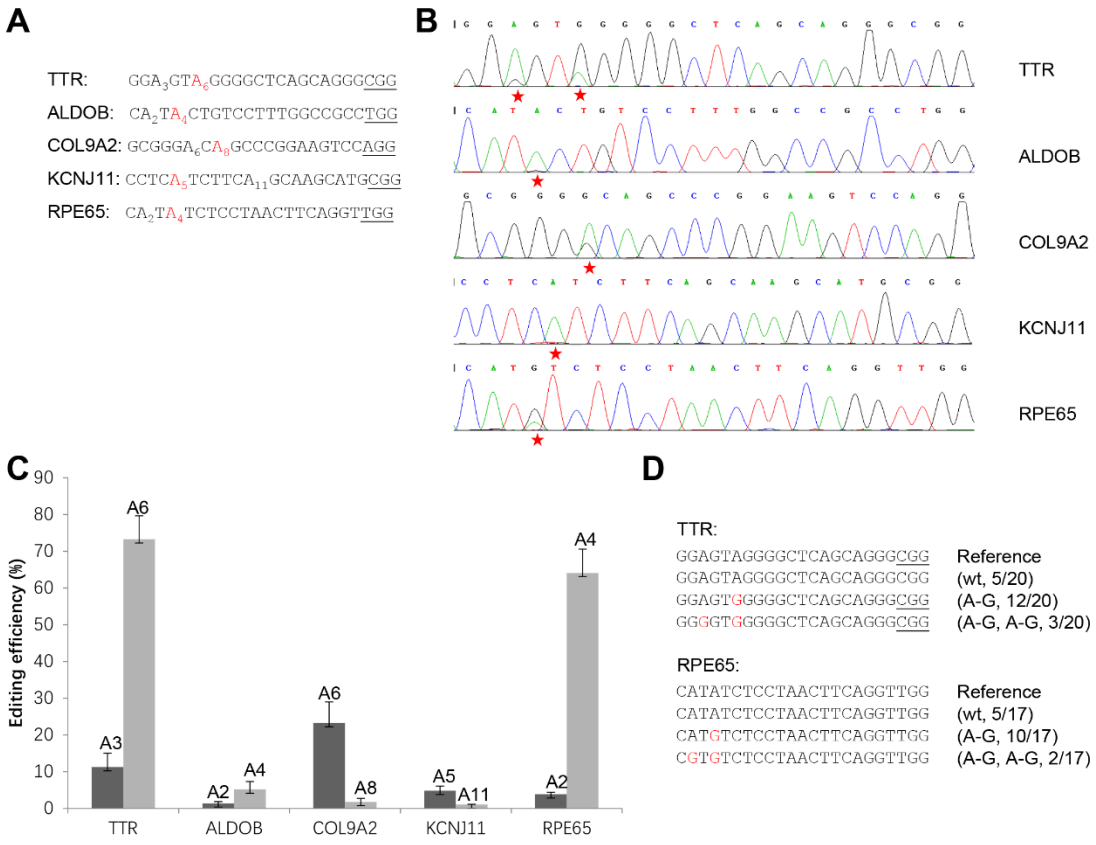

Supplementary Figure 1 Detection of pathogenic A-to-G substitution induced by ABE in cells.

A. The representative pathogenic mutations. Five human genes with reported pathogenic mutation were selected, and the related pathogenic points are highlighted in red. The PAM sequences are underlined.

B. The representative chromatogram of the Sanger sequencing of target sites from genomic DNA of HEK293T cells transfected with ABE and related sgRNAs. The red stars indicate the conversion of A-to-G.

C. The editing efficiency of A-to-G within the target sites. Data from three independent experiments were shown as means ± s.d.

D. Sequences of the PCR product after TA cloning for *TTR* and *RPE65*. The PAM sequences are underlined; the modified bases highlighted in red. N/N indicates bacterial colonies with base editing out of total number of the sequenced bacterial colonies.

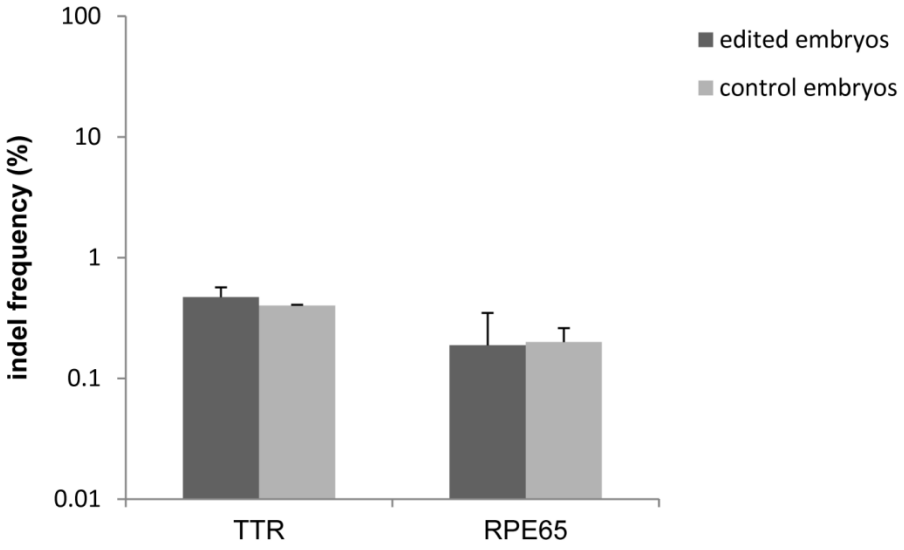

Supplementary Figure 2 Detection of indels for *TTR* and *RPE65*

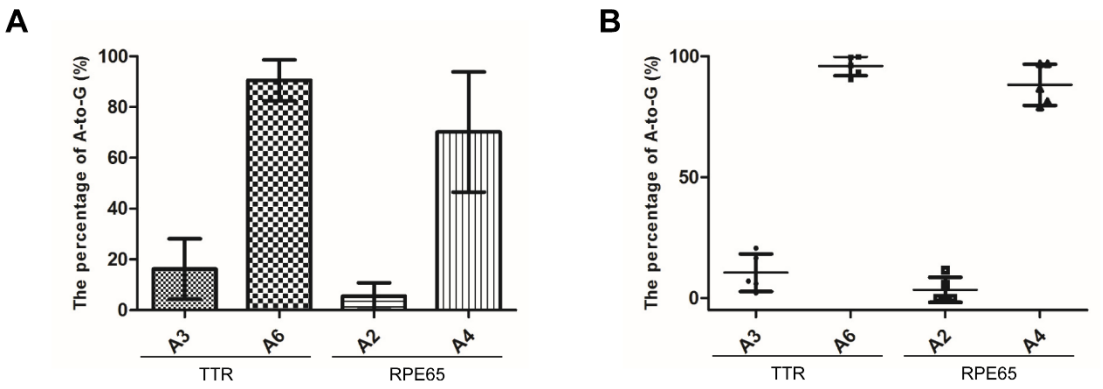

Supplementary Figure 3 Simultaneous editing of multiple sites. A. The editing efficiency was calculated depending on the chromatogram of the Sanger sequencing of target sites. B. The ediitng efficiency was calculated depending on the deep sequencing.

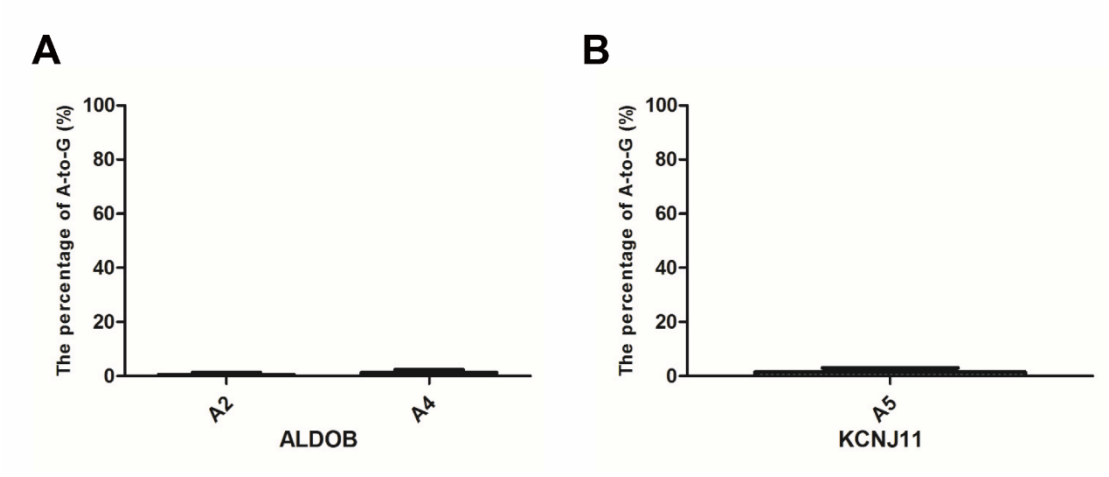

Supplementary Figure 4 The editing efficiency for *ALDOB* and *KCNJ11* in human embryos.

Supplementary Table 1 Summary of the used embryos and editing efficiency

Used sgRNAs	Embryo No.	Editing efficiency（A-to-G）		Used sgRNAs	Embryo No.	Editing efficiency（A-to-G）		Used sgRNAs	Embryo No.	Editing efficiency（A-to-G）	
1. ABE+ SITE6	Position	A3	A7	4. ABE+ COL9A2	Position	A2	A4	8. ABE+ TTR	#68	22%	86%
	#1	7%	41%		#35	8%	55%		#69	14%	89%
	#2	0%	39%		#36	3%	90%		#70	22%	95%
	#3	0%	49%		#37	78%	91%		#71	35%	89%
	#4	0%	60%		#38	37%	100%		#72	2%	94%
	#5[a]	0%	88%	5. ABE+ KCNJ11	Position	A5			#73	7%	98%
	#6	25%	70%		#39	0%			#74	8%	90%
	#7	5%	48%		#40	2%			#75	35%	71%
	#8	45%	65%		#41	0%			#76	5%	98%
	#9	44%	93%		#42	4%			#77	12%	96%
	#10	0%	45%		#43	0%		8. ABE+ RPE65	Positon	A2	A4
	#11	6%	55%		#44	3%			#68	12%	50%
	#12	0%	100%		#45	1%			#69	0%	50%
2. ABE+ SITE2	Position	A2	A5 A8	6. ABE+ TTR	Position	A3	A6		#70	4%	87%
	#13	4%	99% 1%		#46	0%	78%		#71	3%	70%
	#14	4%	100% 3%		#47	80%	90%		#72	1%	98%
	#15	3%	89% 10%		#48	18%	80%		#73	16%	25%
	#16	4%	96% 2%		#49	18%	92%		#74	2%	97%
	#17	3%	99% 8%		#50	13%	88%		#75	3%	60%
	#18	2%	99% 1%		#51	6%	90%		#76	10%	85%
	#19	2%	86% 2%		#52	1%	82%		#77	4%	80%
	#20	6%	91% 3%		#53	2%	95%	9. ABE+ TTR	Position	A3	A6
	#21	3%	50% 16%		#54	35%	86%		#78	14%	95%
	#22	8%	99% 14%		#55	14%	74%		#79	0	96%
	#23	0%	100% 0%		#56	9%	70%		#80	0	80%
	#24	1%	83% 2%		#57	9%	87%		#81	33%	100%
3. ABE+ ALDOB	Position	A2	A4	7. ABE+ RPE65	Position	A2	A4		#82	10%	87%
	#25	0%	2%		#58	12%	60%		#83	30%	89%
	#26	0%	0%		#59	0%	38%	10. ABE-NG+ BCS1L-1	Position	A4	A7
	#27	1%	3%		#60	8%	64%		#85	19%	11%
	#28	2%	1%		#61	1%	42%		#86	26%	15%
	#29	0%	0%		#62	0%	50%		#87	21%	14%
	#30	1%	1%		#63	0%	26%	11. ABE-NG+ BCS1L-2	Position	A5	A7
	#31	0%	2%		#64	0%	70%		#88	42%	24%
4. ABE+ COL9A2	Position	A6	A8		#65	0%	53%		#89	33%	0
	#32	29%	87%		#66	2%	60%		#90	32%	0
	#33	52%	30%		#67	5%	41%				
	#34	36%	48%		Position	A3	A6				

[a] The embryos marked in red were subjected for deep sequencing.

Supplementary Table 2 Summary of the off-target sites for TTR

Position	1	2	3	4	5	6	7	8	9	10	11	12	13	14	15	16	17	18	19	20	N	G	G	Location			
Target site	G	G	A	G	T	A	G	G	G	G	C	T	C	A	G	C	A	G	G	G	C	G	G	Chr.	Strand	Start	End
TTR-OF1	A	G	A	G	T	G	G	G	G	G	C	T	C	A	G	C	A	G	G	G	T	G	G	7	-	101886959	101886981
TTR-OF2	G	G	A	G	C	A	C	A	G	G	C	T	C	A	G	C	A	G	G	G	T	G	G	9	-	134834935	134834957
TTR-OF3	C	G	G	G	C	A	G	G	C	G	C	T	C	A	G	C	A	G	G	G	T	G	G	1	-	54459729	54459751
TTR-OF4	G	G	G	G	G	G	C	G	G	G	C	T	C	A	G	C	A	G	G	G	A	G	G	1	-	233055471	233055493
TTR-OF5	A	G	C	C	T	A	G	G	G	C	C	T	C	A	G	C	A	G	G	G	A	G	G	16	-	3144125	3144147
TTR-OF6	G	C	C	G	T	C	G	G	C	G	C	T	C	A	G	C	A	G	G	G	A	G	G	1	-	217186869	217186891
TTR-OF7	G	C	C	G	G	A	G	G	G	G	C	T	C	A	G	C	A	G	G	G	C	A	G	19	-	35925685	35925707
TTR-OF8	G	G	C	C	A	A	G	G	G	G	C	T	C	A	G	C	A	G	G	G	G	A	G	2	-	16397188	16397210
TTR-OF9	A	G	A	G	C	T	G	G	G	G	C	T	C	A	G	C	A	G	G	G	G	A	G	11	+	119792041	119792063
TTR-OF10	G	G	T	G	T	T	G	G	G	G	C	T	C	A	G	C	A	G	G	G	T	G	G	12	+	68329077	68329099
TTR-OF11	G	G	C	T	C	A	G	G	G	G	C	T	C	A	G	C	A	G	G	G	T	G	G	3	+	129512561	129512583
TTR-OF12	A	G	A	G	T	C	A	G	G	G	C	T	C	A	G	C	A	G	G	G	A	G	G	17	+	18256612	18256634
TTR-OF13	T	G	G	G	C	T	G	G	G	G	C	T	C	A	G	C	A	G	G	G	A	G	G	7	-	1057874	1057896
TTR-OF14	G	T	T	G	A	T	G	G	G	G	C	T	C	A	G	C	A	G	G	G	T	G	G	11	-	2894294	2894316
TTR-OF15	T	T	A	G	G	A	A	G	G	G	C	T	C	A	G	C	A	G	G	G	T	G	G	9	-	136104150	136104172
TTR-OF16	G	G	A	A	T	G	G	A	G	G	C	T	C	A	G	C	A	G	G	G	T	G	G	17	-	17627042	17627064
TTR-OF17	A	C	A	G	C	A	G	T	G	G	C	T	C	A	G	C	A	G	G	G	A	G	G	2	-	199141685	199141707
TTR-OF18	C	C	T	G	T	A	G	G	C	G	C	T	C	A	G	C	A	G	G	G	T	G	G	9	+	137070161	137070183
TTR-OF19	G	C	T	A	T	A	G	A	G	G	C	T	C	A	G	C	A	G	G	G	A	G	G	12	+	12331390	12331412
TTR-OF20	G	T	G	G	T	C	G	A	G	G	C	T	C	A	G	C	A	G	G	G	C	G	G	2	+	120794406	120794428
TTR-OF21	G	T	A	G	A	T	A	G	G	G	C	T	C	A	G	C	A	G	G	G	G	G	G	10	+	13995879	13995901

Supplementary Table 3 Summary of the off-target sites for RPE65

Position	1	2	3	4	5	6	7	8	9	10	11	12	13	14	15	16	17	18	19	20	N	G	G	Location			
target site	C	A	T	A	T	C	T	C	C	T	A	A	C	T	T	C	A	G	G	T	T	G	G	Chr.	Strand	Start	End
RPE65-OF1	C	T	T	G	T	C	T	T	C	A	A	A	C	T	T	C	A	G	G	T	T	A	G	9	-	117426716	117426738
RPE65-OF2	G	G	T	A	T	C	T	T	C	T	A	A	A	T	T	C	A	G	G	T	G	G	G	6	-	106501910	106501932
RPE65-OF3	C	A	G	A	C	C	A	C	C	C	A	A	C	T	T	C	A	G	G	T	G	G	G	3	+	28844733	28844755
RPE65-OF4	G	A	T	C	A	C	T	C	C	T	A	C	C	T	T	C	A	G	G	T	G	G	G	10	+	60419751	60419773
RPE65-OF5	A	A	T	G	G	C	T	C	C	T	A	G	C	T	T	C	A	G	G	T	A	G	G	7	+	119799948	119799970
RPE65-OF6	C	A	T	C	T	G	T	C	C	A	A	G	C	T	T	C	A	G	G	T	G	G	G	15	+	80808417	80808439
RPE65-OF7	C	A	T	C	T	G	T	C	C	T	G	T	C	T	T	C	A	G	G	T	T	G	G	21	-	21012624	21012646
RPE65-OF8	C	A	T	G	A	C	T	A	C	T	A	A	C	C	T	C	A	G	G	T	T	G	G	2	-	20195444	20195466
RPE65-OF9	C	A	T	T	T	C	T	A	C	T	T	A	G	T	T	C	A	G	G	T	A	G	G	14	+	81537161	81537183
RPE65-OF10	G	A	G	A	C	C	T	C	A	T	A	A	C	T	T	C	A	G	G	T	C	A	G	2	-	24436599	24436621
RPE65-OF11	C	A	T	A	G	C	G	A	C	A	A	A	C	T	T	C	A	G	G	T	T	G	G	2	-	173678502	173678524
RPE65-OF12	A	A	T	G	A	A	T	C	C	T	A	A	C	T	T	C	A	G	G	T	G	A	G	14	+	20442316	20442338
RPE65-OF13	G	A	T	A	T	C	T	T	A	A	A	A	C	T	T	C	A	G	G	T	T	G	G	17	-	11634934	11634956
RPE65-OF14	C	C	T	C	C	A	T	C	C	T	A	A	C	T	T	C	A	G	G	T	G	G	G	2	+	218577991	218578013
RPE65-OF15	T	T	T	A	T	T	T	C	C	C	A	A	C	T	T	C	A	G	G	T	A	A	G	20	-	41219765	41219787
RPE65-OF16	C	C	T	G	T	G	T	C	C	A	A	A	C	T	T	C	A	G	G	T	G	G	G	12	-	76712189	76712211
RPE65-OF17	T	A	T	C	C	C	T	C	C	T	A	A	C	T	T	C	A	G	G	A	C	A	G	7	+	82392310	82392332
RPE65-OF18	A	A	T	A	C	C	T	A	C	T	A	A	C	T	T	C	A	G	G	A	T	G	G	3	-	128451040	128451062
RPE65-OF19	C	A	G	A	T	C	T	C	C	T	C	A	A	T	T	C	A	G	G	T	G	G	G	6	+	167581892	167581914
RPE65-OF20	C	C	T	A	C	C	T	C	C	T	T	A	T	T	T	C	A	G	G	T	T	G	G	10	+	69872858	69872880
RPE65-OF21	C	A	C	A	T	A	C	C	C	T	A	T	C	T	T	C	A	G	G	T	A	G	G	16	-	52342604	52342626
RPE65-OF22	G	G	T	T	T	C	A	C	C	T	A	A	C	T	T	C	A	G	G	T	A	G	G	10	-	57853408	57853430
RPE65-OF23	A	A	T	A	A	C	T	A	T	T	A	A	C	T	T	C	A	G	G	T	G	G	G	20	-	32437696	32437718

Supplementary Table 4 Primers used in the study

Primer name	Sequence (5'-3')	Product length (bp)	Usage
TTR-ON-249-F	TTTTTCGGGCTCTGGTG	249	On-target detection
TTR-ON-249-R	TATGAGGTGAAAACACTGCTT		
RPE65-ON-248-F	TGTCATTGCCTGTGCTCA	248	
RPE65-ON-248-R	ACATGAGGCAGGAGGACAA		
COL9A2-ON-269-F	GCCTCTGGATCTCAGTTTC	269	
COL9A2-ON-269-R	ACAGAGTTGGTAACAAGGCA		
KCNJ11-ON-237-F	TCCTGATCCTCATCGTGC	237	
KCNJ11-ON-237-R	TGGTGGTCTTGCGTACCA		
ALDOB-ON-238-F	AGGCAGACAGGGTCAAGG	238	
ALDOB-ON-238-R	GGATTGGAGGAAAAGTTGC		
SITE6-ON-230-F	GGGAAACGCCCATGCAATTA	230	
SITE6-ON-230-R	GTCAACCAGTATCCCGGTGC		
SITE2-ON-236-F	AGCTCCTGAGATACAGTCACGAG	236	
SITE2-ON-236-R	AGCTTCCTGAAATGCTGTGCGTGT		
RPE65-OF1-257-F	CCAGAGCCCACTGATGTTGAT	257	Off-target for RPE65
RPE65-OF1-257-R	AAAGCAGGCTGGGGGGA		
RPE65-OF2-252-F	TGGGCAGTGTATATTAATTGG	252	
RPE65-OF2-252-R	ACAGCTACAGCCAAGTCAGA		
RPE65-OF3-241-F	GACGGTTACCAGAGTGCG	241	
RPE65-OF3-241-R	ATCCCTGTGGCTCTCAATA		
RPE65-OF4-238-F	AGTCCCTTCTCCTGCCTAC	238	
RPE65-OF4-238-R	GAGAAAAGAAAAGCAAGGC		
RPE65-OF5-250-F	TCAACTAATTACTCAAAGAGAAA	250	
RPE65-OF5-250-R	GGACATAAATAAATGCCCTA		
RPE65-OF6-243-F	TTCCACTGCTGAGACCCT	243	
RPE65-OF6-243-R	CCACTGTATCCTGGCTTG		
RPE65-OF7-262-F	ATTTCTACTCCTGGTTTTGC	262	
RPE65-OF7-262-R	CAGAGACCCAAGGAGAGC		
RPE65-OF8-274-F	AAACATCTGAAATGATTCCTAAC	274	
RPE65-OF8-274-R	AGCCATTATCAGTAAACACCTC		
RPE65-OF9-275-F	GTAAATTAAAGTTTTCATGCATA	275	
RPE65-OF9-275-R	CAAACATACTCCTCCACAATC		
RPE65-OF10-250-F	AATGAACAGAAACAACACCTAAG	250	
RPE65-OF10-250-R	TGGCAACAGAGCGAGACT		
RPE65-OF11-246-F	AGACCACTTTTCCTAAGTCACTA	246	
RPE65-OF11-246-R	GAGGAAGAGTCAATAAAATGCT		
RPE65-OF12-267-F	AAGACAGTCTGGGAGGCAA	267	
RPE65-OF12-267-R	TTGGGGTAGTGCCAGAAA		
RPE65-OF13-273-F	CCATACCTGGTCATTCTGC	273	
RPE65-OF13-273-R	CCCTTGCTTTAAGTCAACG		

RPE65-OF14-248-F	CCCCTTTGGTTACTGGATTGT	248	
RPE65-OF14-248-R	GCTTTTTTCCTCCTTTCCCA		
RPE65-OF15-249-F	AGCAAGCCCTATAACTCAAGA	249	
RPE65-OF15-249-R	CTGATAGAGTAGCCGCCAT		
RPE65-OF16-245-F	TTTTAATAGAGACGGGGTTTC	245	
RPE65-OF16-245-R	CCTTCTTGCTATTTGCTGATT		
RPE65-OF17-239-F	CCAACCTTTGAATGATGCC	239	
RPE65-OF17-239-R	AAAAATGAGGTTACTCCGACA		
RPE65-OF18-237-F	TCTTCCCTTCTGCCTCCTGT	237	
RPE65-OF18-237-R	CTGCCATCGCCATCACG		
RPE65-OF19-274-F	CGTGGCTAACTTGACCTCTG	274	
RPE65-OF19-274-R	CTGGGACTGCTACCAATGTG		
RPE65-OF20-234-F	TTGAAACCGTAAGAAGAGCC	234	
RPE65-OF20-234-R	GGGTTTTGAAGGTGGAGC		
RPE65-OF21-244-F	AAATAAATAAATAGCATCCTTCA	244	
RPE65-OF21-244-R	TTCACCTCAGACCAGCCT		
RPE65-OF22-250-F	AAGTATTAGAAGTTTGAGAGAAG	250	
RPE65-OF22-250-R	AAAGTTTTAGCCCTGGTT		
RPE65-OF23-236-F	CCTGAGCTCTCCTGCAAG	236	
RPE65-OF23-236-R	CCCTGTGCTGGCTTCTTT		
TTR-OF1-236-F	ACCTAAATGGGAGGCTTGC	236	Off-target for TTR
TTR-OF1-236-R	AGGACTCAACAACGCCCA		
TTR-OF2-235-F	CAGTGCGTTTCCAGGTAGT	235	
TTR-OF2-235-R	TGGTAGCAGTGGTAGGTGA		
TTR-OF3-242-F	AAATGTGTTTGAAGGAGCGAG	242	
TTR-OF3-242-R	GGGCTGGGACAGACCTCA		
TTR-OF4-236-F	GGAGGAAGCAGCAAAGAAG	236	
TTR-OF4-236-R	CCCACAGGACCACAGACC		
TTR-OF5-265-F	GCCCCGTCTCGCCCTAT	265	
TTR-OF5-265-R	CAGGGCAGTGACTACAGCGG		
TTR-OF6-243-F	TGCCAGGTGACAGTCAGAAC	243	
TTR-OF6-243-R	TATTTAGGGCATCTTGAGTCTCT		
TTR-OF7-235-F	ATCAGCCACCTTGGACAT	235	
TTR-OF7-235-R	TTAGAGTGAGGGTTGAGTTTG		
TTR-OF8-239-F	CAGATGAAGATGGGAGAAAG	239	
TTR-OF8-239-R	GCTACTTCAAAAATACCAGGA		
TTR-OF9-250-F	CAGGACTAGGAGCAAGATTG	250	
TTR-OF9-250-R	GGGGACCTAGCACATTTG		
TTR-OF10-255-F	TTCATCACCTTCCCCTCAA	255	
TTR-OF10-255-R	GGGTGTCCCTGCTTCTCC		
TTR-OF11-242-F	TTCCTTCCAGAGCACTTTC	242	
TTR-OF11-242-R	TCTTCCATTTCAGTCACACC		
TTR-OF12-247-F	GAAGCGTGGTCAGGTTGT	247	

TTR-OF12-247-R	CTATGAGCAGAGCTGGAAGA		
TTR-OF13-265-F	GGAGTGTGGGCGGCGAA	265	
TTR-OF13-265-R	TTCTGCATCTTGGCGCACTC		
TTR-OF14-243-F	CTCAAGAGTTCCAGACCCA	243	
TTR-OF14-243-R	TACAAATAAGACCCCACATAA		
TTR-OF15-258-F	AGTGCCTCTGTGCAGTGGA	258	
TTR-OF15-258-R	TGGGACACCAGTGCTCTCT		
TTR-OF16-246-F	ATAATCCCACTACAGTCCCA	246	
TTR-OF16-246-R	GCTGGTGAGAGCATCCC		
TTR-OF17-258-F	GCCAGGGAAAGCTTGAAG	258	
TTR-OF17-258-R	CCTCTCTACTGGCAGGTCAT		
TTR-OF18-237-F	GGAGCGAACACCAGGCG	237	
TTR-OF18-237-R	CCTGCGCGAGATCGAGTC		
TTR-OF19-257-F	TGATAACGCCGCCTCTCTA	257	
TTR-OF19-257-R	ATTCTCCCTGCCAACCTTT		
TTR-OF20-272-F	AAGGTGAAGGGTTTCCAGT	272	
TTR-OF20-272-R	CTCTGGGTCTTGGCACTT		
TTR-OF21-267-F	TGACATAAGCACACCATTCT	267	
TTR-OF21-267-R	AACTATGAGCAATAAACTTCTGT		